Materials Chemistry and Physics 147 (2014) 636–643

Contents lists available at ScienceDirect

Materials Chemistry and Physics

journal homepage: www.elsevier.com/locate/matchemphys

Nanostructure and mechanical properties of aromatic polyamide and reactive organoclay nanocomposites

Muhammad Usman Alvi [a], Sonia Zulfiqar [b, **], Cafer T. Yavuz [c], Hee-Seok Kweon [d], Muhammad Ilyas Sarwar [a, *]

[a] Department of Chemistry, Quaid-i-Azam University, Islamabad 45320, Pakistan
[b] Department of Chemistry, School of Natural Sciences (SNS), National University of Sciences and Technology (NUST), Islamabad 44000, Pakistan
[c] Graduate School of EEWS, Korea Advanced Institute of Science and Technology, 335 Gwahangno, Yuseong-gu, Daejeon 305-701, Republic of Korea
[d] Division of Electron Microscopic Research, Korea Basic Science Institute, 169-148 Gwahak-ro, Yuseong-gu, Daejeon 305-806, Republic of Korea

HIGHLIGHTS

- Surface modification of montmorillonite was carried out with *p*-phenylenediamine.
- Aromatic polyamide with carbonyl chloride chain ends was synthesized.
- Compatibility between the clay and polyamide was achieved by surface modification of MMT.
- TEM micrographs confirmed successful fabrication of the nanocomposites.
- Results indicated the improvements in thermal and mechanical profile of the materials.

GRAPHICAL ABSTRACT

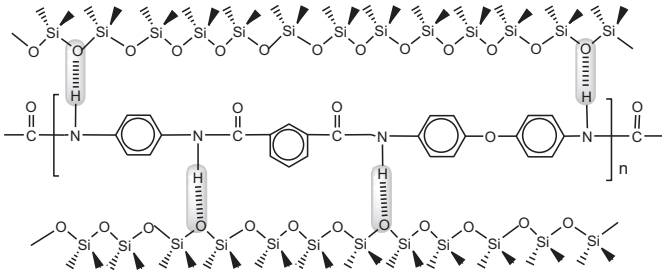

ARTICLE INFO

Article history:
Received 9 March 2013
Received in revised form
14 March 2014
Accepted 2 June 2014
Available online 20 June 2014

Keywords:
Composite materials
Polymers
Electron microscopy
Mechanical testing

ABSTRACT

Aromatic polyamide/organoclay nanocomposites were synthesized using the solution blending technique. Treatment of montmorillonite clay with *p*-phenylenediamine produced reactive organophilic clay for good compatibility with the matrix. Polyamide chains were prepared by condensing a mixture of 1,4-phenylenediamine and 4-4′-oxydianiline with isophthaloyl chloride under anhydrous conditions. These chains were end capped with carbonyl chloride using 1% extra acid chloride near the end of reaction to develop the interactions with organoclay. The dispersion and structure–property relationship were monitored using FTIR, XRD, FE-SEM, TEM, DSC and tensile testing of the thin films. The structural investigations confirmed the formation of delaminated and disordered intercalated morphology with nanoclay loadings. This morphology of the nanocomposites resulted in their enhanced mechanical properties. The tensile behavior and glass transition temperature significantly augmented with increasing organoclay content showing a greater interaction between the two disparate phases.

1. Introduction

Polymeric composites are extensively employed in a variety of applications involving construction, transportation and electronics. The properties of these materials are strongly influenced by the size, shape, dimension, volume fraction and microstructure of the

* Corresponding author. Tel.: +92 51 90642132; fax: +92 51 90642241.
** Corresponding author. Tel.: +92 301 5017753; fax: +92 51 90855552.
E-mail addresses: soniazulfiqar@yahoo.com (S. Zulfiqar), ilyassarwar@hotmail.com (M.I. Sarwar).

http://dx.doi.org/10.1016/j.matchemphys.2014.06.001
0254-0584/

reinforcing phase. The true polymer/clay nanocomposites can be traced back to the work of Toyota group on the exfoliation of clay platelets in the polyamide-6 matrix [1–3]. These materials demonstrated a substantial improvement of many engineering properties by reinforcing polyamides with clay on the nanometer scale [4,5]. Tensile modulus of polyamide-6 was increased two folds by addition of 5–6 wt. % nanolayers relative to glass fibers whereas, three times this amount of glass fibers required to achieve the same increase [6,7]. The first commercial relevance of these nanocomposites was the development of timing belt covers for Toyota cars and later on, these polyamide-6/clay nanocomposites were used as engine covers [8,9]. Polyamide-6,6/clay nanocomposites were prepared by the compounding method [10]. TEM micrographs revealed an exfoliated morphology of the materials and tensile strength increased from 75 (polyamide-6,6) to 81 MPa up to 1.6-wt. % clay content. Polyamide-6,6/clay nanocomposites have also been fabricated using clay co-intercalated with quaternary ammonium salt and epoxy resin [11]. The exfoliation was confirmed using XRD and TEM with improvement properties. These nanocomposites containing 5-wt. % clay showed improvements in tensile strength from 78 (polyamide-6,6) to 98 MPa, notched Izod strength from 96 to 146 Jm^{-1}, and HDT from 75 to 164 °C. Wu et al. reported exfoliated polyamide-10,12 obtained by condensation polymerization with increased strength and gas barrier properties [12]. Liu and coworkers reported the preparation of exfoliated polyamide-11/clay nanocomposites with excellent mechanical and thermal properties [13], while polyamide-12/clay hybrid materials were developed for automotive fuel lines and fuel system components.

The improvement has important implications since lower filler content render into low density materials needed for much relevance, especially in aerospace and transportation. In space shuttle, such low density materials give extra-advantage over the space machinery made up of conventional materials. In automobile, where fuel efficiency is important these materials again have promising benefits over the common materials. Additionally, aliphatic polyamide/clay composites have been used to improve barrier resistance in beverage and packaging applications. Aliphatic-aromatic polyamide (Nylon MXD6) prepared from m-xylylenediamine and adipic acid, has a high gas barrier property compared with polyamide-6 or polyamide-6,6. Nylon MXD6-clay nanocomposites demonstrated exfoliated morphology with high gas barrier properties [14] and these nanocomposites are suitable for drink bottles. Multi-layer PET/MXD6-clay nanocomposite bottle has a shelf life seven times as long as a PET bottle and three times as long as a multi-layer PET/MXD6 bottle. This development has been extended to other engineering polymers including aliphatic polyamides [15,16], polystyrene [17–19], polymethylmethacrylate [20], polyacrylate [21], polycarbonate [22], epoxies [23–25], polysulfone [26], polyurethane [27], polyaniline [28], aromatic polyamides [29,30] and polyimides [31,32]. The aliphatic polyamides/clay nanocomposites have thoroughly been studied but aromatic polyamides have not been paid much attention in this area.

Aromatic polyamides are recognized for their outstanding properties in terms of thermal stability, mechanical properties, high glass temperature and good resistance to solvents. Owning to their high performance and superb properties, aromatic polyamides [33–36] and their composites [33] are frequently exploited for defense and aerospace applications. However, these polymers suffer solubility problems as matrices for organoclay nanocomposites and difficult to process due to their infusibility and poor solubility in organic solvents. To make them more tractable and soluble for advanced applications is to lower the glass transition temperature (T_g) and softening point (T_s) by the incorporation of flexible, bulky substituents as pendent groups or using meta linkages along the backbone of such polymers. These groups enhance the solubility, processability and toughness of the polymers without sacrificing their thermal properties. Nowadays, clay nanocomposites, especially based on polyamides along with other [37,38] have attracted much attention because these hybrids have tremendous applications in coating, flame retarding, barrier and electronic materials [39–42].

Keeping in view the importance of the nanocomposites, a soluble aromatic polyamide was prepared by the reaction of diamines (*p*-phenylenediamine and 4,4′-oxydianiline) with isophthaloyl chloride using N,N-dimethylacetamide as solvent. These polymer chains were endcapped with carbonyl chloride groups using a slight excess of the acid chloride. Montmorillonite clay was modified with the ammonium salt of *p*-phenylenediamine. The amine end group of swelling agent was changed into cations to interact chemically with the negatively charged silicate layers while free amine end group reacted with the acid chloride groups of the polyamide chains diffused into the space between nanolayers. The compatibility between the two phases was achieved through swelling agent thus rendering more permanent effect due to the larger number of polyamide chains connected to the organoclay. Thin nanocomposite films obtained by evaporation of the solvent were characterized using FTIR, XRD, SEM, TEM, DSC and tensile testing.

2. Experimental

2.1. Materials

1,4-phenylenediamine ≥ 99%, 4,4′-oxydianiline ≥ 98%, isophthaloyl chloride ≥98%, triethylamine ≥99% and hydrochloric acid >99% were obtained from Fluka and used as such. N,N-dimethylacetamide (DMAc) > 99%, silver nitrate > 99% and montmorillonite (MMT) K-10 (cation exchange capacity 119 meq/100 g) having chemical composition SiO_2 (43.77%), Al_2O_3 (18.57%), CaO (1.02%), Na_2O (1.13%) and H_2O (36.09%) [43] were obtained from Aldrich and used as received.

2.2. Synthesis of polyamide matrix

A mixture of 1,4-phenylenediamine and 4-4′-oxydianiline was placed in the reaction flask along with the addition of DMAc as a solvent under an inert atmosphere. To the above amine solution, a stoichiometric amount of isophthaloyl chloride was added to the flask under anhydrous conditions. The contents of the flask were cooled below 0 °C to avoid any side reaction due to exothermicity of the polymerization reaction and then it was allowed to come to ambient temperature after 1 h. The reaction between diamines and diacid chloride is fast; even then the reaction mixture was agitated for 24 h for its completion [35]. A stoichiometric amount of triethylamine was used to remove HCl produced as precipitates. The polyamide resin obtained was golden yellow in color (Scheme 1). In order to create interactions between aromatic polyamide and nanoclay, the aromatic polyamide chains were end capped with carbonyl chloride groups using 1% extra diacid chloride at a later stage.

2.3. Preparation of organically modified montmorillonite (OMMT)

Montmorillonite was organically modified by ion exchange method in aqueous medium using *p*-phenylenediamine. The swelling agent was placed in a beaker containing water, followed by the addition of stoichiometric amount of concentrated hydrochloric acid. The solution was heated at 80 °C. In a separate beaker, MMT was dispersed in water at 80 °C and then mixed with ammonium

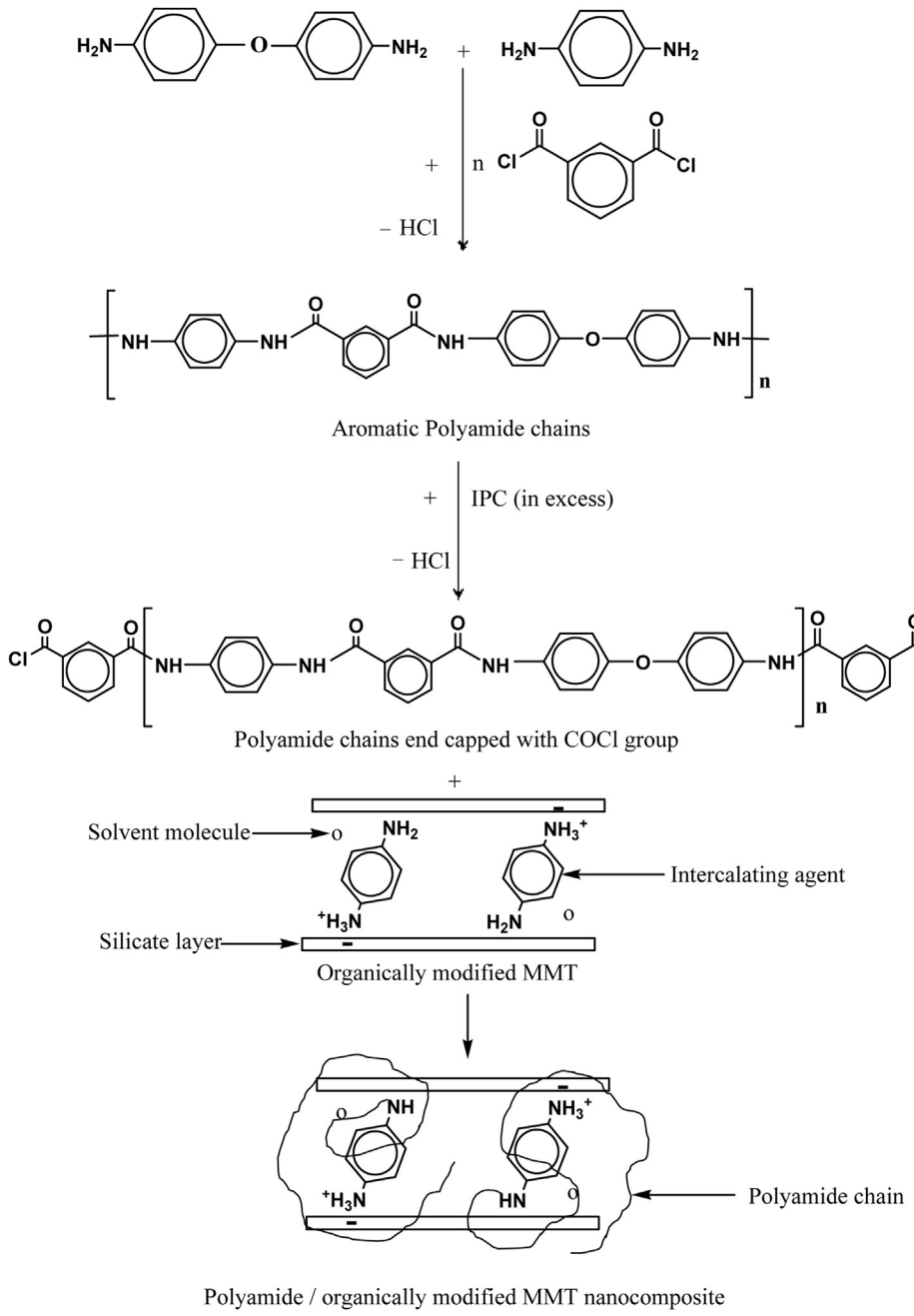

Scheme 1. Schematic representation for the formation of carbonyl chloride end-capped polyamide chains and polyamide/OMMT nanocomposites.

salt of *p*-phenylenediamine with vigorous stirring for 3 h at 60 °C. The precipitates were isolated by filtration and were washed with hot water and filtered again. This process was repeated thrice to remove the residual amount of swelling agent. The filtrate was titrated with $AgNO_3$ until there were no AgCl precipitates to ensure a complete removal of chloride ions. The final product obtained by filtration was dried in a vacuum oven at 80 °C for 24 h. The dried cake was grounded to fine powder and exploited for the preparation of nanocomposites.

2.4. Preparation of nanocomposite films

For the preparation of nanocomposites, a measured amount of polyamide solution was transferred to flask and then a known quantity of nanoclay was added for a particular concentration (Scheme 1). The mixture was agitated at a high speed for 24 h at room temperature for homogeneous dispersion of nanolayers in the polymer matrix. Similarly the nanocomposites with varying concentrations (2–10 wt. %) were prepared by mixing different amounts of clay to the polyamide solution. Hybrid films of uniform thickness were obtained by pouring the above prepared concentrations into petri dishes placed on a leveled surface. The solvent was evaporated and thin films obtained were further dried at 60 °C under vacuum to a constant weight.

2.5. Characterization

The synthesized polyamide matrix, neat MMT, OMMT and thin films of nanocomposites were analyzed using Excalibur series Thermo Nicolet 6700 FTIR spectrophotometer, over the range of

4000–500 cm^{-1}. Inherent viscosity (η_{inh}) was measured in DMAc at 30 °C with an Ubbelohde viscometer using polymer concentration of 0.5 g dL^{-1}. The diffraction pattern of the related materials was recorded with the help of X-ray diffractometer 3040/60 XPert PRO PAN analytical in reflection mode (radiation wavelength = 0.154 nm) with scanning angle range $2\theta = 2°$ to 10°. For phase morphological studies, composite films were cryogenically fractured in liquid nitrogen and the morphology was observed with the help of FEI Nova 230 field emission scanning electron microscope whereas the internal morphology of ultramicrotomed samples was investigated using FEI Tecnai G^2 Spirit Twin transmission electron microscope, operated at an accelerating voltage of 120 kV. Mechanical properties of the rectangular strips with dimensions (ca. 14 × 5.0–7.4 × 0.20–0.39 mm^3) were measured according to DIN procedure 53455 at 25 °C using Testometric Universal Testing Machine M350/500. To determine various mechanical properties, standard procedures and formulae were used and an average value obtained from 5 to 7 different measurements in each case has been reported. The glass transition temperatures of nanocomposites were characterized using a NETZSCH DSC 204 F1 differential scanning calorimeter using 5–10 mg of samples encapsulated in aluminium pans and heated at a ramp rate of 10 °C min^{-1} under nitrogen atmosphere.

3. Results and discussion

Inherent viscosity of polyamide measured at a concentration of 0.05 g dL^{-1} in DMAc at 30 °C was 1.01 dL g^{-1} η_{inh}, as a good criterion for the assessment of molecular weight, revealed reasonably high molecular weight of the synthesized polyamide relative to the reported values for other aromatic polyamides [44]. Pristine aromatic polyamide film was transparent and golden yellow in color. This color was changed to black upon the addition of organoclay. Thin films (0.20–0.39 mm ± 0.02) prepared from polyamide containing up to 10-wt. % organoclay were black in color, transparent at low concentrations of organoclay and the films containing 10-wt. % clay content were semitransparent. Various techniques employed for the characterization of these nanocomposite materials are described below.

3.1. FTIR analysis

IR spectra of pure polyamide matrix, neat MMT, OMMT and nanocomposite film in both lowest and highest wave numbers are represented in Figs. 1 and 2 respectively. The N–H stretching and bending vibrations appeared at 3245 cm^{-1} and 1607 cm^{-1}. The aromatic C–H stretching at 3061 cm^{-1} while aromatic C=C stretching vibrations at 1539 cm^{-1} and 1495 cm^{-1} were also observed. The C=O stretching of polyamide appeared at 1644 cm^{-1} and broadening of the band showed the C=O in different environments, i.e., amide C=O, both free and combined. The bands at 1214 cm^{-1} and 1075 cm^{-1} described the C–O–C asymmetric and symmetric stretching. Montmorillonite gave most intense band at 1015 cm^{-1} corresponding to Si–O stretching of silicate layers whereas bands at 3625 cm^{-1} and 796 cm^{-1} assigned to the stretching and bending vibrations of O–H group confirming the presence of hydroxyl groups attached on clay layers. The bands at 3366 cm^{-1} and 1632 cm^{-1} attributed to O–H stretching and bending of water molecules adsorbed in interlayer spacing of clay.

Organically modified montmorillonite gave two additional bands at 3012 cm^{-1} and 1515 cm^{-1} representing the aromatic C–H stretching and N–H bending of aromatic diamine, thus verifying the intercalation of clay layers with aromatic diamine. Nanocomposite films showed characteristic bands of both matrix and the reinforcement i.e., bands at 3245 cm^{-1} and 1607 cm^{-1} designated to the N–H stretching and bending while the stretching vibrations due to aromatic C–H and C=C appeared at 3051 cm^{-1}, 1539 cm^{-1} and 1496 cm^{-1} respectively for polyamide matrix. The bands at 1645 cm^{-1} for C=O and at 1232 cm^{-1} and 1080 cm^{-1} for C–O–C asymmetric and symmetric stretching were also observed. A stretching vibration at 1012 cm^{-1} for Si–O confirmed the presence of silicate layers in the nanocomposites.

3.2. X-ray diffraction

Dispersion of the OMMT in the polyamide matrix was scrutinized by XRD patterns taken at low 2θ region and the data are shown in Fig. 3. The pure MMT gave a (001) reflection at $2\theta = 8.82°$, which matched to a basal spacing of 1.0 nm. The OMMT used for the

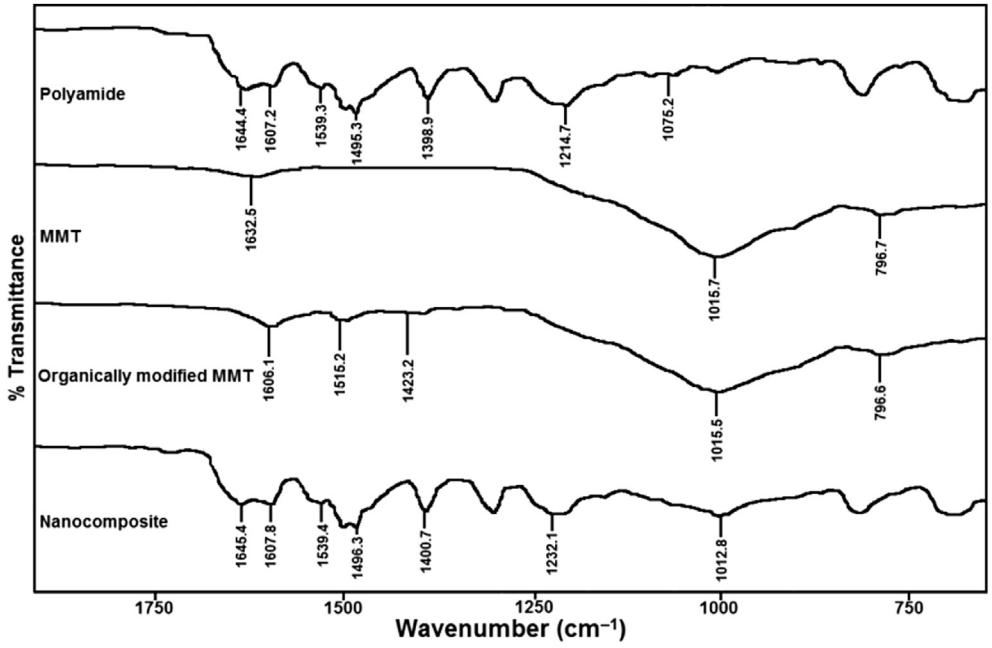

Fig. 1. FTIR spectra of pure polyamide, MMT, OMMT and polyamide/OMMT nanocomposites at lowest wave number.

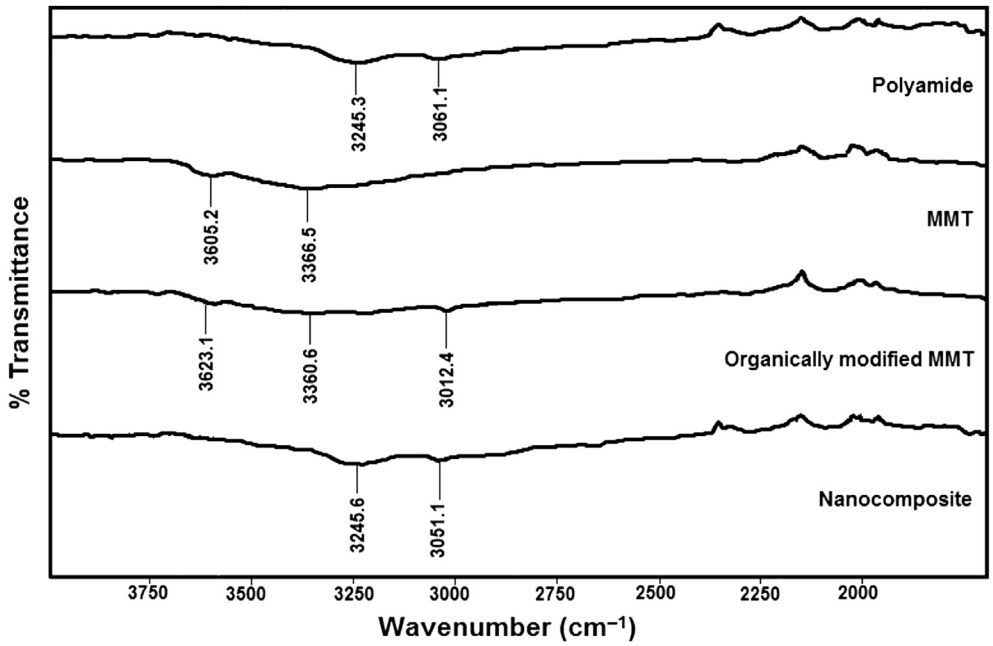

Fig. 2. FTIR spectra of pure polyamide, MMT, OMMT and polyamide/OMMT nanocomposites at highest wave number.

production of nanocomposites indicated a shift in (001) reflection towards lower angle at $2\theta = 5.98^\circ$ ($d = 1.476$ nm). This increase in d-spacing was due to the replacement of small sized Na^+ ions with large sized cationic aromatic diamine confirming the intercalation of clay. In the nanocomposites containing 2–10 wt. % OMMT, the peak appearing at $2\theta = 5.98^\circ$ ($d = 1.476$ nm) was gone indicating dispersion of ordered platelets of nanolayers and authenticated delamination of OMMT in the polyamide matrix (Fig. 3). However, XRD results provide incomplete information about the extent of dispersion and contain no peak regarding nanoclay delamination.

Dispersion of clay in the composites depends on the type of intercalating agent and its subsequent interaction with the matrix. The cationic end of swelling agent interacted with silicate layers through electrostatic forces and other free amine group develops interactions with carbonyl chloride end-capped polyamide chains diffused into the interlayer of OMMT. These interactions result a finite interlayer expansion of clay when polyamide chains intercalated between the nanolayers. Thus, polyamide's transitional entropy increases while its conformational entropy decreases, but simultaneously, OMMT gains conformational entropy. The fine

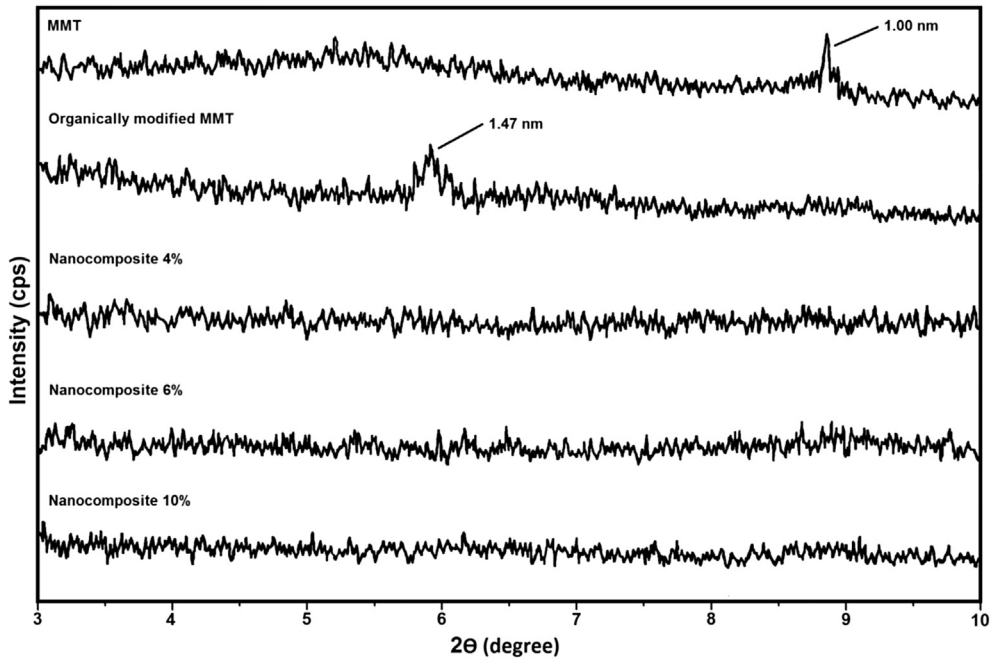

Fig. 3. XRD patterns of pure MMT, OMMT and polyamide/OMMT nanocomposites.

dispersion of nanolayers depends on both entropic and enthalpic contributions of the system, which are related to the properties of polymer and modified clay. Polyamide being a polar polymer made the enthalpic translation between the polymer and OMMT much easier so that the chains of polyamide intercalated between the nanolayers of clay.

3.3. Morphological studies

Field emission scanning electron microscopy provides information about the surface morphology of the materials and FESEM micrographs of nanocomposite films with 2 and 6-wt. % of clay in polyamide matrix are shown in Fig. 4. The morphology indicated a good dispersion of the clay layers in the whole polyamide matrix without agglomeration to any one place. So, the results supported the idea of changing the nature of the clay from hydrophilic to organophilic for better dispersion in order to get nanocomposites rather than conventional composites. The interlayer spacing of silicate layers in the original clay and in the polymer-organoclay nanocomposites were determined conventionally by XRD.

On the other hand, internal morphology of the nanocomposites was observed by using TEM. It allows a qualitative understanding of the internal structure through direct observations. Fine dispersion of nanolayers in the polyamide/OMMT nanocomposites can be seen more clearly through TEM micrographs as given in Fig. 5. The dark lines of micrograph are usual 1 nm thick clay layers; the spaces between the dark lines are interlayer spaces and a gray base is the polyamide matrix. Polyamide/OMMT nanocomposites containing low clay content showed good dispersion in the polymer matrix (Fig. 5(a)) giving delaminated morphology. With the addition of 6-wt. % OMMT in the composites, clay dispersed well in the matrix as depicted from Fig. 5(c) beyond agglomeration may start that deteriorate the properties of the nanocomposites. These images showed intercalation of clay because small sized Na^+ ion exchanged with large sized cationic *p*-phenylenediamine, as a result of which distance between clay stacking had increased and insertion of polyamide chains occurred in between clay nanolayers along with some disturbance in the layered structure of clay. These results are in perfect agreement with results of XRD analysis as shown in Fig. 3.

3.4. Tensile testing

Mechanical properties of the nanocomposites indicate how the material would respond to forces, being applied in tension. Stress–strain curves and the related mechanical properties of nanocomposites containing different percentages of OMMT are given in Fig. 6 and Table 1. The data indicate that tensile strength of the composite materials enhances with increasing organoclay content. The value obtained for pure polyamide was 42 MPa, which improved to 89 MPa for the nanocomposites containing 6-wt. % clay. The tensile moduli for pristine polyamide obtained from the stress–strain data had a value of 2.54 GPa that increased to a maximum value 3.95 GPa with 6-wt. % organoclay and then it

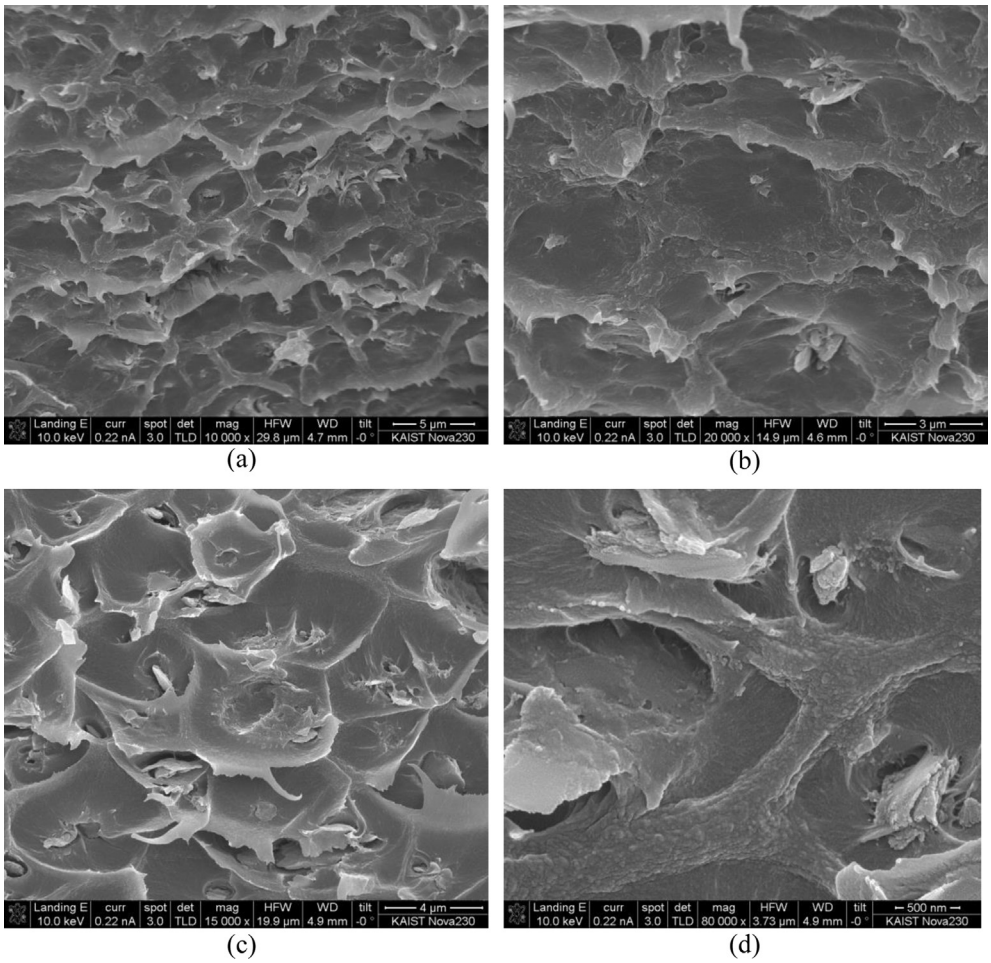

Fig. 4. FESEM micrographs of polyamide/OMMT nanocomposites (a & b) 2-wt. % (c & d) 6-wt. %.

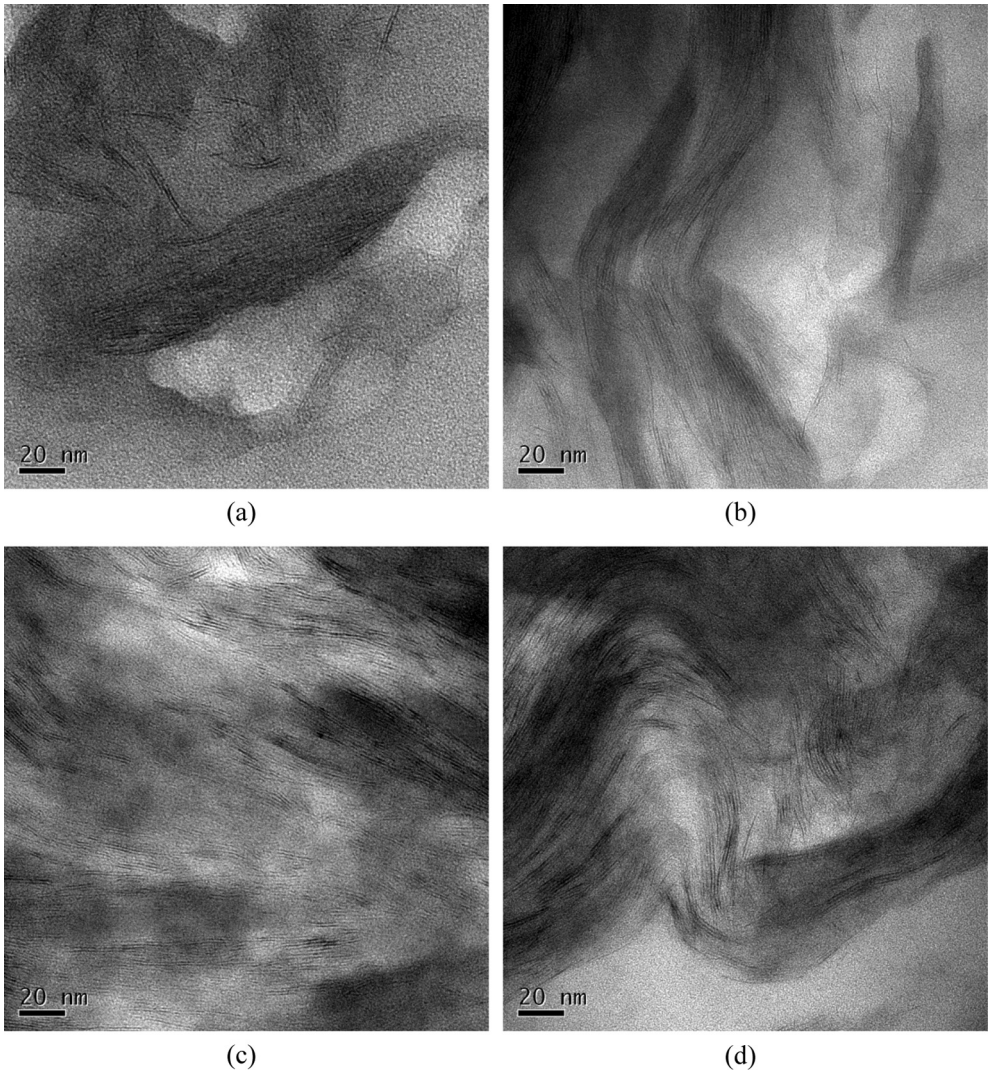

Fig. 5. TEM micrographs of polyamide/OMMT nanocomposites (a & b) 2-wt. % (c & d) 6-wt. %.

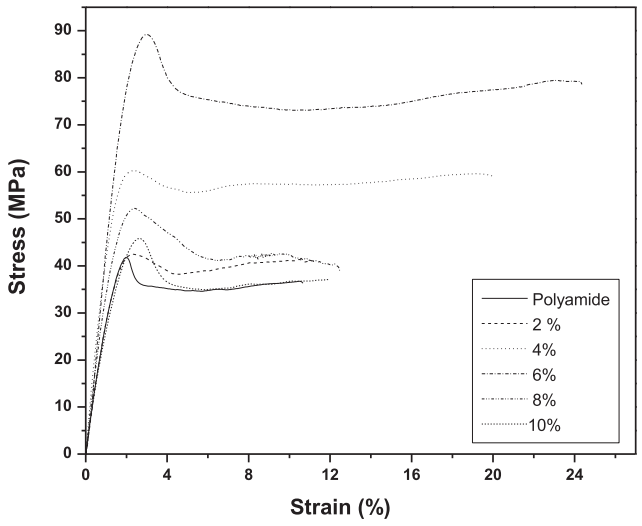

Fig. 6. Stress–strain curves of polyamide/OMMT nanocomposites.

deceased. The elongation at break point and toughness initially increased and then decreased with the addition of higher amount of OMMT. These results revealed improvements in the mechanical properties of the nanocomposites as compared to pristine polyamide, because when nanolayers were introduced in small amounts, these distributed themselves in the form of fine platelets and the stress was more efficiently transferred from the matrix to the reinforcement via strong interactions between the polyamide and OMMT. However, when concentration of inorganic reinforcement increased beyond certain limit, then phase separation occurred which resulted in poor interfacial interactions between

Table 1
Mechanical data of polyamide/OMMT nanocomposites.

Clay loading (%)	Max. Stress (MPa)	Max. Strain (%)	Toughness (MPa)	Young's modulus (GPa)
0	42 ± 0.98	11 ± 0.03	361 ± 0.3	2.54 ± 0.01
2	42 ± 1.0	11 ± 0.03	427 ± 0.2	2.75 ± 0.02
4	60 ± 0.74	20 ± 0.01	1120 ± 0.1	3.59 ± 0,03
6	89 ± 0.65	24 ± 0.02	1794 ± 0.1	3.95 ± 0.02
8	51 ± 1.02	12 ± 0.02	520 ± 0.2	2.97 ± 0.01
10	46 ± 1.01	11 ± 0.01	409 ± 0.4	2.37 ± 0.03

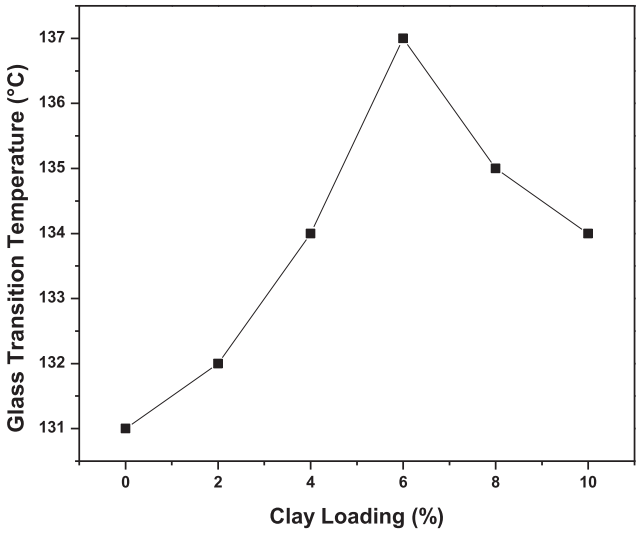

Fig. 7. Variation of glass transition temperatures as a function of clay loading in the nanocomposites.

the two disparate phases. This non homogeneous distribution of the nanolayers in the matrix increased the number of defects or flaws in the material and was responsible for brittleness and deterioration in the mechanical properties of nanocomposites.

3.5. *Differential scanning calorimetry*

Polymers usually act as glassy solids below their glass transition temperatures with no segmental mobility. Polymer passed through glassy to rubbery region when heated. This transition is actually known as the glass transition temperature and can be followed by differential scanning calorimetry (DSC). The glass transition data is presented in Fig. 7. These results described an increase in the T_g values with increasing organoclay content, which showed a greater interaction of the two disparate phases. The maximum increase in the T_g value (137 °C) was observed with 6-wt. % addition of organoclay than the pure polyamide (131 °C) and then decreased with higher content of the clay. Organoclay reduced the segmental motion of the polymer chains and with increasing proportion of the inorganic phase shifted T_g towards higher temperature. This implied that polyamide chains linked with OMMT. Therefore, the motion of polymer chains was restricted at higher OMMT concentrations raising the T_g values of the nanocomposites. These increases relative to pure polyamide were due to the intercalation of the polymer chains into the interlayer of OMMT suppressing the mobility of polymer segments near the interface. The rigid amorphous component of the nanocomposites increases with augmenting OMMT content, thereby, reducing the segmental mobility significantly. In this way, chains immobilization takes place when they are intercalated between the nanolayers shifting the T_g towards higher temperature [45].

4. Conclusions

The incorporation of organoclay reinforced the polyamide matrix, describing ample compatibility between the two phases. Chemical interaction produced among the composite components resulted in uniformly dispersed OMMT throughout the matrix. At 6-wt. % OMMT loading, the distribution of clay platelets was optimum thus yielding increased mechanical profile of these materials. At 8-wt. % clay loading and beyond, it might be existed in the form of clusters that had less cohesion with polyamide and adversely affected the mechanical properties. At higher concentration of clay, the layers might be stacked together, impeding further inclusion of the chains between the layers, thus degrading the properties of composites. The glass transition temperatures of nanocomposites were also improved with the addition of the clay content in the polyamide matrix.

Acknowledgments

The authors appreciate the financial support provided by the Higher Education Commission of Pakistan (HEC) through project research grant 20-23-ACAD (R) 03-410 and acknowledge the cooperation of Electron Microscopic Research Team especially Hye-Jin Cho, Korea Basic Science Institute, Daejeon, Republic of Korea.

References

[1] Y. Fukushima, S. Inagaki, J. Incl. Phenom. 5 (1987) 473.
[2] A. Usuki, M. Kawasumi, Y. Kojima, A. Okada, J. Mater. Res. 8 (1993) 1174.
[3] A. Usuki, Y. Kojima, M. Kawasumi, A. Okada, Y. Fukushima, T. Kurauchi, O. Kamigaito, J. Mater. Res. 8 (1993) 1179.
[4] Y. Kojima, A. Usuki, M. Kawasumi, A. Okada, Y. Fukushima, T. Kurauchi, O. Kamigaito, J. Mater. Res. 8 (1993) 1185.
[5] P.B. Messersmith, E.P. Giannelis, J. Polym. Sci. A Polym. Chem. 33 (1995) 1047.
[6] C.L. Tucker III, E. Liang, Compos. Sci. Technol. 59 (1999) 655.
[7] D.A. Brune, J.U. Bicerano, Polymer 43 (2002) 369.
[8] T. Kurauchi, A. Okada, T. Nomura, T. Nishio, S. Saegusa, R. Deguchi, SAE Tech. Paper Series, SAE, Detroit, 1991, Feb, 910584.
[9] A. Okada, J. Miner, Met. Mater. Soc. 45 (1993) 71.
[10] M. Kato, H. Okamoto, N. Hasegawa, A. Usuki, N. Sato, in: Proc. 6th Japan Int. SAMPE, 1999, p. 693.
[11] X. Liu, Q. Wu, Macromol. Mater. Eng. 287 (2002) 180.
[12] Z. Wu, C. Zhou, R. Qi, H. Zhang, J. Appl. Polym. Sci. 83 (2002) 2403.
[13] T. Liu, K.P. Lim, W.C. Tjiu, K.P. Pramoda, Z.K. Chen, Polymer 44 (2003) 3529.
[14] K. Maruo, Advance in Polymeric Nanocomposites, CMC Publishers, Tokyo, 2004, p. 54.
[15] A. Okada, M. Kawasumi, A. Usuki, Y. Kojimi, T. Kurauchi, O. Kamigato, Mater. Res. Symp. Proc. 171 (1990) 45.
[16] B. Hoffmann, J. Kressler, G. Stopplemann, C. Friedrich, G.-M. Kim, Colloid Polym. Sci. 278 (2000) 629.
[17] J.W. Gilman, C.L. Jackson, A.B. Morgan, R. Harris Jr., E. Manias, E.P. Giannelis, M. Wuthenow, D. Hilton, S.H. Philips, Chem. Mater. 12 (2000) 1866.
[18] X. Fu, S. Qutubuddin, Polymer 42 (2001) 807.
[19] C.I. Park, O.O. Park, J.G. Lim, H.J. Kim, Polymer 42 (2001) 7465.
[20] D.C. Lee, L.W. Jang, J. Appl. Polym. Sci. 61 (1996) 1117.
[21] Z. Chen, C. Huang, S. Liu, Y. Zhang, K. Gong, J. Appl. Polym. Sci. 75 (2000) 796.
[22] X. Huang, S. Lewis, W.J. Brittain, R.A. Vaia, Macromolecules 33 (2000) 2000.
[23] C. Zilg, R. Mulhaupt, J. Finter, Macromol. Chem. Phys. 200 (1999) 661.
[24] Y. Ke, J. Lu, X. Yi, J. Zhao, Z. Qi, J. Appl. Polym. Sci. 78 (2000) 808.
[25] X. Kornmann, H. Lindberg, L.A. Berglund, Polymer 42 (2001) 4493.
[26] G.S. Sur, H.L. Sun, S.G. Lyu, J.E. Mark, Polymer 42 (2001) 9783.
[27] Y. Hu, L. Song, J. Xu, L. Yang, Z. Chem, W. Fan, Colloid Polym. Sci. 279 (2001) 819.
[28] J. Lu, X. Zhao, J. Mater. Chem. 12 (2002) 2603.
[29] S. Zulfiqar, Z. Ahmad, M. Ishaq, M.I. Sarwar, Mater. Sci. Eng. A 525 (2009) 30.
[30] S. Zulfiqar, M.I. Sarwar, Solid State Sci. 11 (2009) 1246.
[31] T. Agag, T. Koga, T. Takeichi, Polymer 42 (2001) 3399.
[32] H.L. Tyan, Y.C. Liu, K.H. Wei, Chem. Mater. 11 (1999) 1942.
[33] S. Zulfiqar, Z. Ahmad, M.I. Sarwar, Polym. Adv. Technol. 19 (2008) 1720.
[34] S. Zulfiqar, I. Lieberwirth, M.I. Sarwar, Chem. Phys. 344 (2008) 202.
[35] S. Zulfiqar, M.I. Sarwar, High. Perform. Polym. 21 (2009) 3.
[36] S. Zulfiqar, M. Ishaq, M.I. Sarwar, Adv. Polym. Technol. 29 (2010) 300.
[37] A. Sarfaraz, M.F. Warsi, M.I. Sarwar, M. Ishaq, Bull. Mater. Sci. 35 (2012) 539.
[38] U. Nadeem, Z. Ahmad, S. Zulfiqar, M.I. Sarwar, J. Appl. Polym. Sci. 126 (2012) 1814.
[39] T.D. Fornes, P.J. Yoon, H. Keskkula, D.R. Paul, Polymer 42 (2001) 09929.
[40] S. Zulfiqar, I. Lieberwirth, Z. Ahmad, M.I. Sarwar, Acta. Mater. 56 (2008) 4905.
[41] L.M. Liu, Z.N. Qi, X.G. Zhu, J. Appl. Polym. Sci. 71 (1999) 1133.
[42] S. Zulfiqar, M. Ishaq, M.I. Sarwar, Surf. Interface Anal. 40 (2008) 1195.
[43] Z. Wei, J.M. Moldowan, A. Paytan, Org. Geochem 37 (2006) 891.
[44] Y. Kasashima, T. Kaneda, F. Akutsu, K. Naruchi, M. Miura, Polym. J. 26 (1994) 1179.
[45] C.E. Corcione, A. Maffezzoli, Thermochim. Acta 485 (2009) 43.